

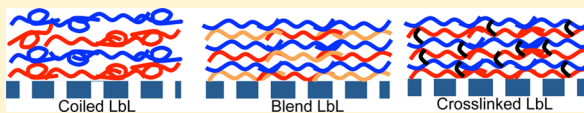
## Spray Assembled, Cross-Linked Polyelectrolyte Multilayer Membranes for Salt Removal

Kwun Lun Cho,<sup>†</sup> Hannah Lomas,<sup>†</sup> Anita J. Hill,<sup>‡</sup> Frank Caruso,\*<sup>†</sup> and Sandra E. Kentish\*,<sup>†</sup>

<sup>†</sup>Department of Chemical and Biomolecular Engineering, The University of Melbourne, Parkville, VIC 3010, Australia

<sup>‡</sup>CSIRO – Materials Science and Engineering, Clayton, VIC 3169, Australia

**ABSTRACT:** The present study reports the synthesis of spray-coated cross-linked polyelectrolyte multilayer membranes. Membrane cross-linking was performed using alkyne-azide “click” chemistry, where alkyne and azide functional groups were used to modify the poly(acrylic acid) (PAA) and the poly(allylamine) hydrochloride (PAH) polyelectrolytes. The results demonstrate that deposition at lower ionic strength produced smoother and denser membrane structures. Pore size analysis using neutral poly(ethylene glycol) revealed a decrease in the membrane pore size as the degree of cross-linking was increased, resulting in the membrane rejecting divalent  $\text{CaCl}_2$  at levels of up to 80%, and 50% rejection of monovalent  $\text{NaCl}$ . When poly(sodium-4-styrenesulfonate) (PSS) was combined with small amounts of cross-linkable PAA, significant flux increases were observed in the multilayer membranes with no observable reduction in ion rejection.

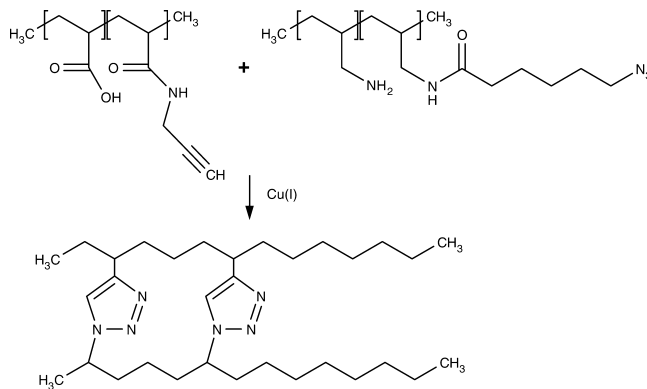


### INTRODUCTION

The efficient production of clean water for drinking and irrigation purposes is of significant economic and environmental importance.<sup>1</sup> Membrane-based water purification technologies have emerged as economically viable alternatives to thermal distillation purification.<sup>2,3</sup> Desalination membranes are typically asymmetric and generally comprise three distinct layers: (i) a permeable polyester support, (ii) a microporous polysulfone support layer, and (iii) a thin “selective” layer. The overall membrane needs to be relatively thick to withstand the hydraulic pressures that are applied to overcome the osmotic pressure gradient. However, to simultaneously achieve both a high water flux and a high salt selectivity, the active layer of the membrane needs to be thin (less than 100 nm thickness for high water flux), defect-free (for high salt rejection), preferably charged (to assist in salt reduction), and sufficiently hydrophilic (to achieve high water flux). To date, a number of polymeric materials have been utilized as the barrier layer of desalination membranes, where the most common materials are cellulose acetate<sup>4,5</sup> (CA) or polyamides (PA).<sup>6,7</sup> However, these materials have associated limitations in use, such as a narrow operable pH range (CA) and susceptibility to biofouling (CA) and chlorine degradation (PA).<sup>8,9</sup>

Layer-by-layer (LbL) polyelectrolyte multilayer membrane fabrication is an attractive fabrication strategy because of the large variety of charged polymers that can be utilized in LbL assembly.<sup>10,11</sup> Additionally, the membrane structure can be readily tailored by altering the polymer deposition conditions.<sup>12</sup> This method of sequentially depositing polycation and polyanion pairs has already been extensively investigated for pervaporation, nanofiltration (NF), solvent resistant nanofiltration (SRNF), reverse osmosis (RO), gas separation, and forward osmosis (FO) applications.<sup>13–21</sup> Recent studies of the approach also report the cross-linking of polyelectrolyte multilayer membranes through

**Scheme 1. Covalent Cross-linking of PEM Films Using a CuAAC to Form 1,2,3-triazole Linkages between Alkyne and Azide Moieties on PAA and PAH Polymer Chains, Respectively**



either chemical or thermal post-treatments.<sup>22,23</sup> Cross-linking is important because it lowers film swelling, thereby enhancing the mechanical stability of the membrane and the salt rejection without significantly lowering the water flux.<sup>24</sup>

In this paper, we explore the formation of polyelectrolyte multilayer membranes, comprising different blend compositions of both weak (PAA) and strong (polystyrenesulfonate) polyelectrolytes, on porous membrane supports. By varying the blend composition and the ionic strength at deposition, we show that it is possible to tailor properties such as the film pore size and the surface charge. This study therefore provides

**Received:** May 13, 2014

**Revised:** July 7, 2014

**Published:** July 18, 2014

important information on the optimization of LbL membrane fabrication techniques for water treatment membranes as well as providing new insights into the types of cross-linking mechanisms.

Cross-linking of the membranes during polyelectrolyte deposition was achieved via the deposition of "click"-modified

polyelectrolytes, eliminating post-fabrication treatment.<sup>25,26</sup> To the best of our knowledge, this is also the first example that uses a "click" chemistry approach to form cross-linked polyelectrolyte multilayer membranes for a desalination application. In the "click" chemistry approach presented here, weak polyelectrolytes functionalized either with alkyne or azide groups were used, allowing for the covalent cross-linking of adsorbed polymers using a Cu(1)-catalyzed alkyne-azide cycloaddition (CuAAC) to form 1,2,3-triazoles.<sup>26</sup> This technique is particularly versatile, due to the specificity and efficiency of the CuAAC reaction and the ability to cross-link the polymer layers at room temperature in an aqueous environment and in the presence of oxygen. The ease and efficacy of cross-linking has previously been reported.<sup>25,26</sup>

The membranes presented in the current study were fabricated using a spray LbL technique. The spray LbL technique is significantly faster and can also result in the formation of more uniform films than the films that are generated by dip-coating.<sup>27,28</sup> Spraying the polyelectrolyte solutions results in the generation

**Table 1. Molecular Weight Cutoff (MWCO) Values of Polyelectrolyte Membranes**

ionic strength (M)	MWCO (Da)	MWCO (Da)		
		%PAA	non-cross-linked	cross-linked
0	971	0	972	973
0.2	1051	20	1208	1065
0.5	1440	40	2166	995
1	1983	60	2232	973
2	2230	80	20 037	
		100	27 019	627

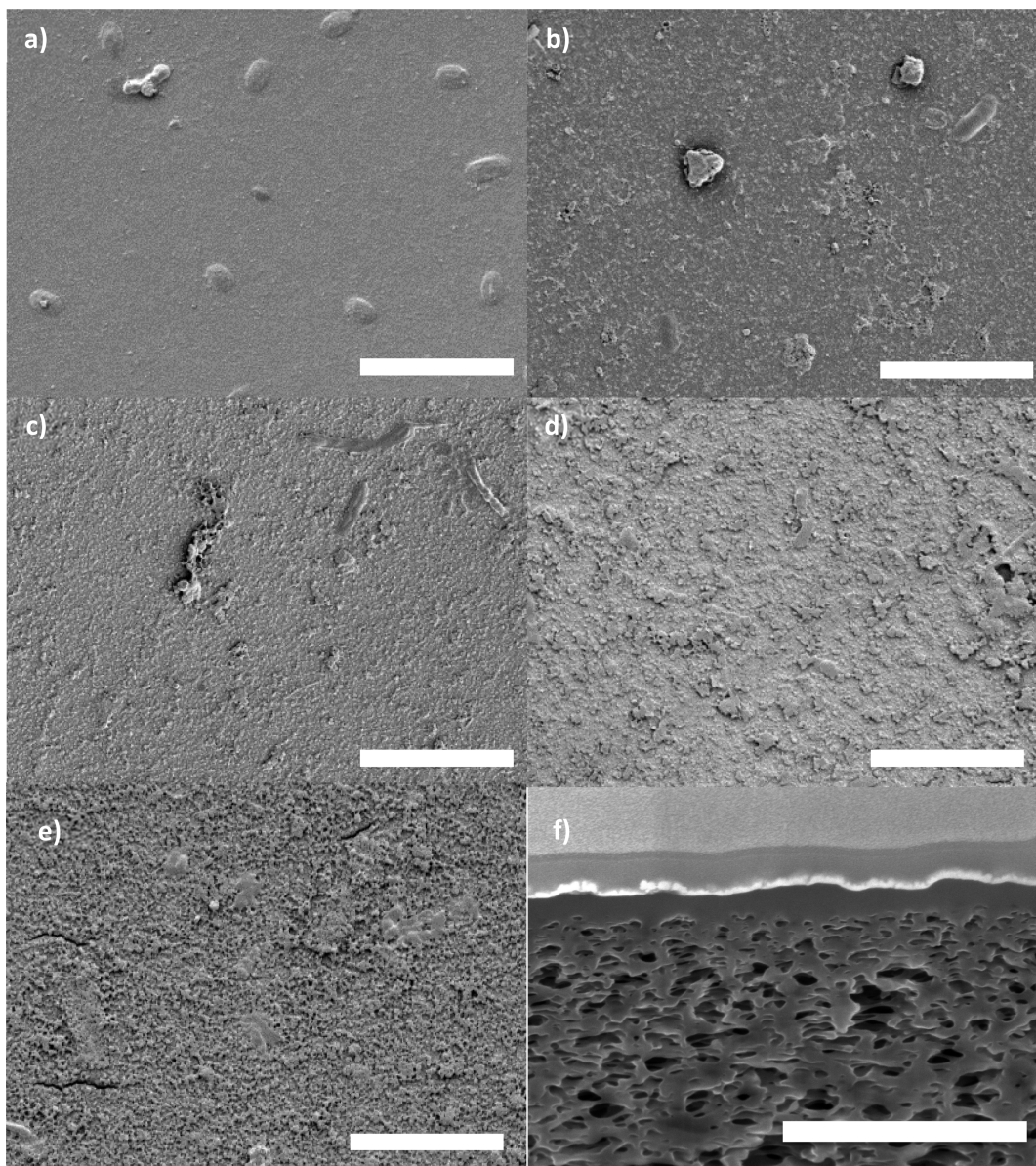


**Figure 1.** SEM images of precompacted  $(\text{PSS}/\text{PAH})_{10}$  membranes deposited in (a) 0 M, (b) 0.2 M, (c) 0.5 M, (d) 1 M, and (e) 2 M NaCl solutions. (f) Cross-sectional SEM image of a multilayer membrane. Scale bars = 1  $\mu\text{m}$ .

of a fine mist that can be introduced evenly and simultaneously onto the entire substrate before the solution is quickly drained away. Thus, polymer chains are kinetically trapped at the point of contact with the substrate.<sup>28</sup> The use of such an approach makes membrane fabrication applicable to production on an industrial scale, as well as being a suitable method for ensuring deposition on a single side of the substrate in comparison with conventional dip-coating.

## EXPERIMENTAL SECTION

**Materials.** Polyethylenimine (PEI,  $M_w \sim 25\,000$ ), poly(sodium-4-styrenesulfonate) (PSS,  $M_n \sim 70\,000$ ), poly(acrylic acid) sodium salt (PAA, 35% solution in water,  $M_n = 60\,000$ ), poly(allylamine hydrochloride) (PAH,  $M_n \sim 70\,000$ ), 4-(4,6-dimethoxy-1,3,5-triazin-2-yl)-4-methylmorpholinium chloride (DMTMM, >96%), propargylamine hydrochloride (95%), sodium azide, 6-bromo hexanoic acid (97%), propionic acid (95%), sodium L-ascorbate (>98%), copper(II) sulfate (>99%), poly(ethylene glycol) ( $M_n \sim 200$ ), poly(ethylene glycol) ( $M_n \sim 300$ ), and poly(ethylene glycol) ( $M_n \sim 1000$ ) were purchased from Sigma-Aldrich. Sodium chloride and calcium chloride were purchased from ChemSupply. All chemicals were used as received. Type A-1 PSF UF membrane substrates (MWCO ~ 92.5 kDa) were kindly provided by General Electric (Fairfield, CT).<sup>29</sup> Commercial gravity fed pressure spray guns (Austech Industries, Australia) were purchased from Autobahn.

**Polyelectrolyte Functionalization: Alkyne-Functionalized Polyacrylic Acid (PAA<sub>alk</sub>).** PAA (1.17 mmol, 300 mg) was dissolved in Milli-Q water (60 mL). DMTMM (3.13 mmol, 865 mg) and propargylamine hydrochloride (0.625 mmol, 57.2 mg) were added to the aqueous solution and allowed to react overnight at room temperature under stirring. The functionalized polymer solution was purified by dialysis for 3 days using a cellulose dialysis membrane (MWCO ~ 3500 kDa) in Milli-Q water and freeze-dried to give a white solid. <sup>1</sup>H NMR (400 MHz, D<sub>2</sub>O, δH) ppm: 1.35–1.55 (CH<sub>2</sub>, polymer), 1.55–1.7 (CH, polymer), 1.9–2.1 (alkyne CH, pendant), 2.2–2.5 (NHCH<sub>2</sub>, pendant). The degree of functionalization was determined to be ~15% by <sup>1</sup>H NMR analysis.

**Polyelectrolyte Functionalization: Azide-Functionalized Poly(allylamine) Hydrochloride (PAH<sub>az</sub>).** PAH (6.30 mmol, 600 mg) was dissolved in Milli-Q water (60 mL). DMTMM (4.80 mmol, 1330 mg) and 6-bromo-hexanoic acid (1.00 mmol, 187 mg) were added to the polymer solution and allowed to react overnight at room temperature under stirring. The bromo-functionalized polymer was purified by dialysis for 3 days using a cellulose dialysis membrane (MWCO ~ 3500 kDa) in Milli-Q water. Sodium azide (0.962 mmol, 62.5 mg) was added to the purified polymer solution and stirred overnight at room temperature away from light to facilitate substitution of the bromo groups with azide groups. The resultant PAH<sub>az</sub> was purified by freeze-drying. <sup>1</sup>H NMR (400 MHz, D<sub>2</sub>O, δH): 1.1–1.5 CH<sub>2</sub> (polymer), 1.7–2.0 CH (polymer), 2.0–2.2 (CONH, pendant), 2.6–3.0 (NH<sub>2</sub>CH<sub>2</sub>, pendant), 3.1–3.4 (CH<sub>2</sub>N<sub>3</sub>, pendant). The degree of functionalization was determined to be ~10% by <sup>1</sup>H NMR analysis.

**Membrane Fabrication.** Flat sheet polysulfone-polyester substrates were cut in 20 × 20 cm<sup>2</sup> squares and stored in Milli-Q water overnight prior to film deposition. Polyelectrolyte films were deposited via spray-coating using a commercially available paint spray gun held ~30 cm from the polysulfone substrate.

In a typical fabrication procedure, the substrate was first coated with a 10 mL aliquot of aqueous PEI solution (1 mg/mL), followed by alternating 10 mL aliquots of a polyanion solution (PSS and/or PAA, 1 mg/mL) and polycation solution (PAH, 1 mg/mL). Polyanion layers containing PAA were deposited at pH = 3.5, adjusted using 1 M HCl, to facilitate increased adsorption. A waiting period of 15 min was allowed between each layer to facilitate adsorption, followed by the rinsing off of excess polyelectrolytes by spraying the surface with ~20 mL of Milli-Q water. A total of 10 bilayers (i.e., PSS/PAH pair) were coated for each membrane sample. Tests were performed to show that membranes consisting of 10 bilayers exhibited the most

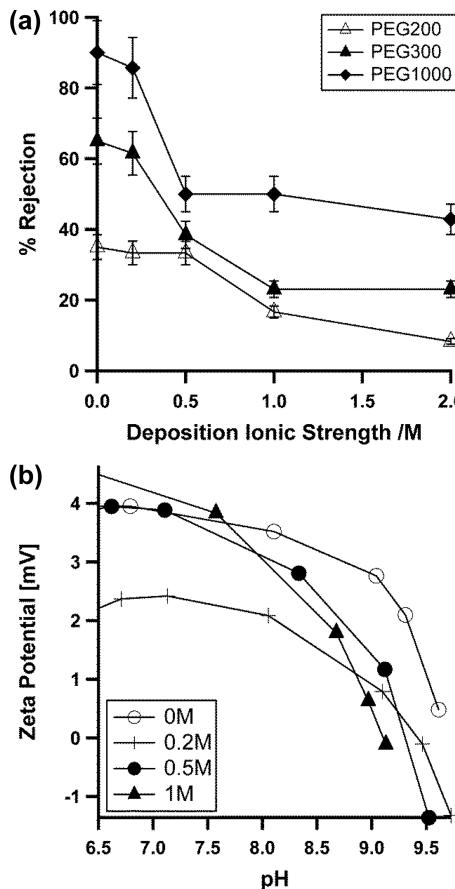


**Figure 2.** (a) Rejection of uncharged PEG with  $M_w = 200$  Da (Δ), 300 Da (▲), or 1000 Da (◆). (b) Streaming potential measurements of LbL membranes deposited at various ionic strengths.

stable water flux and salt rejection results. Variability in performance of membranes with less than 10 bilayers was attributed to possible defects in the ultrathin active layer. Coated membranes were cut into 4.7 cm diameter coupons for characterization and rejection experiments.

**Covalent "Click" Cross-Linking of the Multilayer Films.** Cross-linked membranes were fabricated by depositing the azide/alkyne modified polyelectrolyte solutions with added Cu(I) to facilitate the formation of 1,2,3-triazole linkages between adjacent polymer layers, as shown in Scheme 1. A 10 mL aliquot of a mixture containing CuSO<sub>4</sub> (1.75 g/L), sodium ascorbate (4.4 g/L), and modified polyelectrolyte (1.6 mg/mL) at a ratio of 1:1:3 (v/v/v) was deposited via spray-coating with a 20 min interval between each layer to allow for triazole linkage formation. During this time, the membrane was covered because of the sensitivity of sodium ascorbate to light. This mixture was brown/orange in color as the Cu(II) was reduced to Cu(I) by sodium ascorbate. Excess polyelectrolyte was removed by spraying of ~20 mL of Milli-Q water before the deposition of the next layer. Membranes were then stored in fresh purified water at 4 °C until use.

**Membrane Characterization.** Membrane surface morphologies were observed with a Philips XL30 field-emission scanning electron microscope (SEM). All samples were precompacted under Milli-Q water at 1000 psi before analysis. Membrane surface charge was measured using an Anton-Paar electrokinetic analyzer (Anton-Paar GmbH, Austria) in a 1 mM NaCl solution at pH values ranging from 6 to 9, as adjusted with NaOH. Each data point represents an average of four measurements. The streaming-potential was determined using the Helmholtz-Smoluchowski equation.

For solute rejection and flux experiments, membranes were cut into 4.7 cm diameter circular coupons for insertion into a dead-end filtration cell (Sterlitech HP4750), with an active membrane area of 14.6 cm<sup>2</sup>. All membranes were compacted overnight at 1000 psi in Milli-Q water

prior to testing. Flux and solute rejection experiments were conducted at 800 psi at ambient temperature (20–25 °C). Note that the use of a dead-end filtration cell may lead to lower salt rejection and flux values than could be achieved in a crossflow arrangement due to concentration polarization. The mass transfer coefficient in the concentration polarization boundary layer was determined from the Sutzkover method<sup>30</sup> using a commercial membrane operated at variable salt concentrations, but the same operating pressure, as  $k_{cp} = 1.0 \pm 0.3 \times 10^{-5}$  m/s. The porosity of the active layer of the coated membranes was estimated by assessing the rejection of aqueous PEG solutions (10 mg/mL) of different molecular weights, based on the assumption that hydrated PEG is approximately spherical and that its Stokes radius is dependent on the molecular weight. The Stokes radii ( $a$ ) of the PEG molecules was calculated according to the following equation:<sup>31</sup>

$$a = 4.9 \times 10^{-4} M^{0.672} \quad (1)$$

The concentrations of the PEG in the feed and permeate solutions were determined by refractive index (RI) measurements compared to a calibration chart. The rejection of PEG was defined as

$$\text{rejection} = \left( 1 - \frac{C_p}{C_f} \right) \quad (2)$$

where  $C_p$  and  $C_f$  are the PEG concentrations in the permeate and feed solutions, respectively. Molecular weight cutoff, shown in Table 1, was estimated by extrapolating the molecular weight of PEG solution to achieve 90% rejection according to a literature reported method.<sup>29</sup>

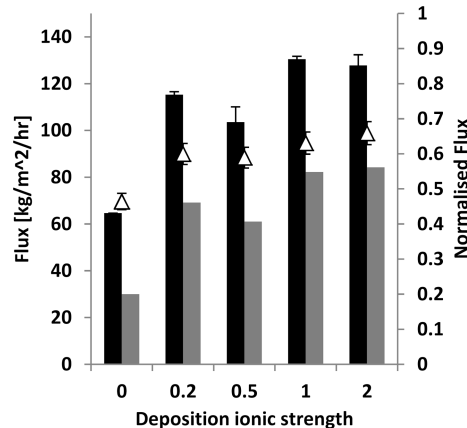


**Figure 3.** Fresh water (black columns), seawater (gray columns), and normalized (open triangles) flux of polyelectrolyte multilayer membranes deposited at various ionic strengths.

Single salt rejection experiments were conducted on NaCl (32 g/L) and CaCl<sub>2</sub> (2 g/L) solutions under constant stirring to reduce concentration polarization. An initial clean water flux test was performed before salt rejection experiments. The mass of permeate collected over time was recorded using an Ohaus Pioneer balance, and the flux was calculated from this mass data. The conductivity of both the feed and permeate solutions were measured, and the apparent rejection calculated as per eq 2. The true rejection of NaCl was also estimated by the determination of the osmotic pressure on the membrane surface ( $\pi_m$ ) by<sup>30</sup>

$$\pi_m - \pi_p = \Delta P \left[ 1 - \frac{J_{\text{salt}}}{J_{\text{water}}} \right] \quad (3)$$

where  $\pi_p$  is the osmotic pressure of the permeate solution,  $J_{\text{salt}}$  is the seawater flux, and  $J_{\text{water}}$  is the freshwater flux. The true rejection is then given by

$$\text{rejection} = \left( 1 - \frac{C_p}{C_m} \right) \quad (4)$$

## RESULTS AND DISCUSSION

**Deposition Ionic Strength.** PSS/PAH membranes were fabricated at different ionic strengths by varying the salt concentration in the deposition solution from 0 to 2 M NaCl. The increase in the solution ionic strength enhances the charge screening of the adsorbing polyelectrolytes, which other workers have shown results in coiled polymer structures<sup>32</sup> and increases the free volume within the polyelectrolyte layers. However, it has also been shown that the deposition of a final layer at high ionic strengths leads to increased surface charge from the greater concentration of coiled polymers, which also results in increased salt rejection.<sup>33,34</sup> As shown in Figure 1, a membrane that is formed at increasing ionic strengths results in a rougher film. The rougher surface may suggest greater disorder within the entire membrane film, implying a greater free volume within the membrane. This is supported by the results shown in Figure 2a, where the membrane rejection of uncharged PEG molecules decreases rapidly with increasing deposition ionic strength, suggesting an increased fractional free volume. Molecular weight cutoff of the membranes, as shown in Table 1, extrapolated using the PEG rejection measurements are also consistent with an increase in free volume within the active layer. Interestingly,

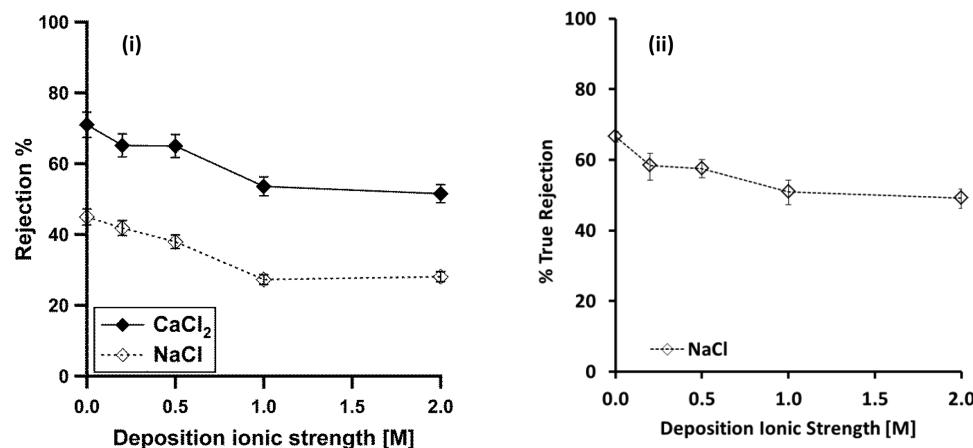


**Figure 4.** Apparent (i) and true (ii) rejection of monovalent NaCl (white) and divalent CaCl<sub>2</sub> (black) for multilayer membranes prepared at various ionic strengths.

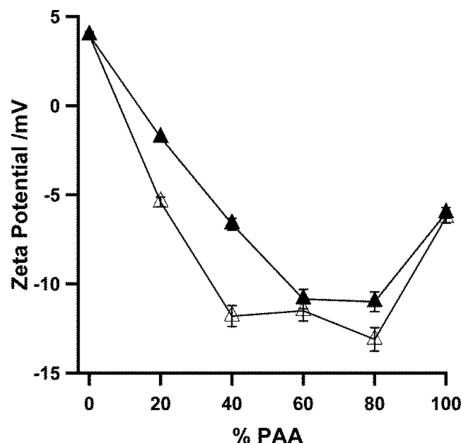


**Figure 5.** Membrane streaming potential at pH 7 as a function of PAA content in the polyanion blend of non-cross-linked ( $\Delta$ ) and cross-linked ( $\blacktriangle$ ) membranes.

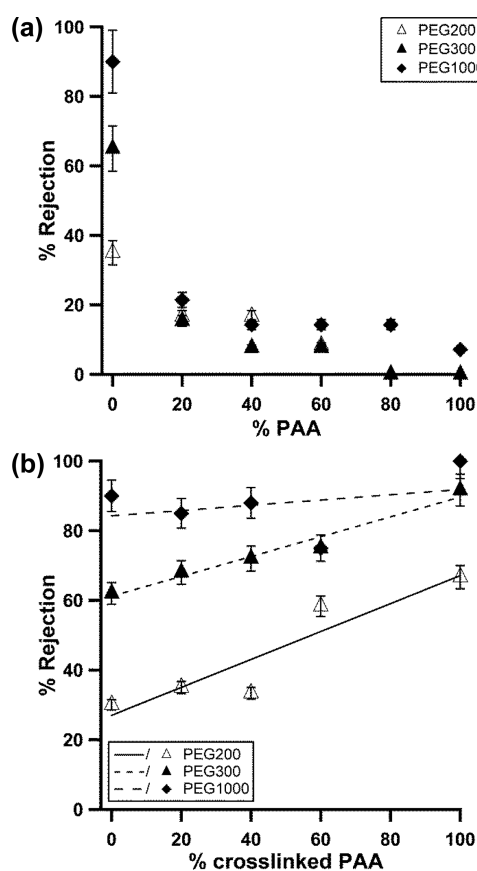


**Figure 6.** Membrane rejection of uncharged PEG at pH 7 on (a) non-cross-linked and (b) cross-linked polyelectrolyte multilayer membranes fabricated with PSS/PAA polyanion blends.

Figure 2b shows that the surface potential for membranes deposited at different ionic strengths changes negligibly.

As shown in Figure 3, a general trend of increasing flux is observed for both fresh water and seawater solutions when the deposition ionic strength is increased. Similarly, normalizing the seawater flux with the fresh water values to eliminate variations in samples gives a minor increase. A greater seawater to fresh water flux ratio reflects a lower osmotic pressure on the surface of the membrane, as shown by eq 3, and thus a fall in the salt rejection. This decreased salt rejection was confirmed in the

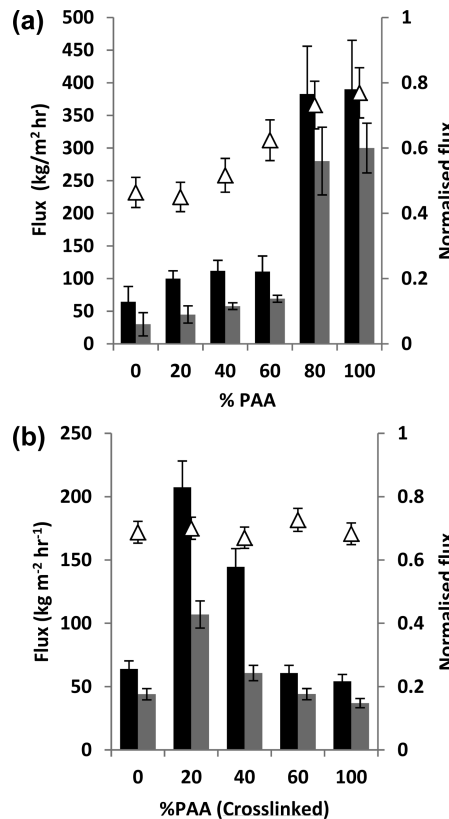


**Figure 7.** Fresh water (black columns), seawater (gray columns), and normalized (open triangles) flux of non-cross-linked (a) and cross-linked (b) membranes fabricated with PSS/PAA polyanion blends.

rejection measurements of both monovalent and divalent salts, as shown in Figure 4. The clear decrease in both the apparent and true rejection with increasing deposition ionic strength is in agreement with the rejection of neutral PEG molecules that indicate an increased free volume within the polymer structure. Although the deposition of a final polyelectrolyte layer at increased ionic strength has been shown to improve membrane performance by increasing the surface charge through polyelectrolyte coiling,<sup>33</sup> the data suggest that bulk film formation is preferably conducted at low or zero ionic strength, which forms more dense polymer layers.

**Cross-Linked Polyelectrolyte Blends.** As shown in Figure 5, the polyelectrolyte membranes become more negatively charged with an increasing PAA content in the polyanion blend. This is attributed to the fact that at lower pH, during deposition ( $\text{pH} = 3.5$ ), protonation of PAA results in less polymer charge and increased PAA adsorption. However, under membrane testing conditions ( $\text{pH} = 7$ ), deprotonation of PAA results in an increased negative charge. The more neutral charge found on the 100% PAA membranes suggests a cooperative adsorption in PSS/PAA polyanion blends favoring PAA via polymer entanglement. Such a phenomenon is not unexpected, as Quinn et al.<sup>35</sup> reported that the composition of polyelectrolyte blend films varied from the blend stoichiometry in solution. However, as shown in Figure 6a, the increase in PAA content also results in a significant decrease in the rejection of neutral PEG molecules, because the deposition of PAA at lower pH ( $\text{pH} \sim 3.5$ ) results in adsorption of coiled polymer chains, causing an increase in free volume.

To facilitate interlayer cross-linking, alkyne-modified PAA ( $\text{PAA}_{\text{alk}}$ ) was also used as the polyanion and compared to

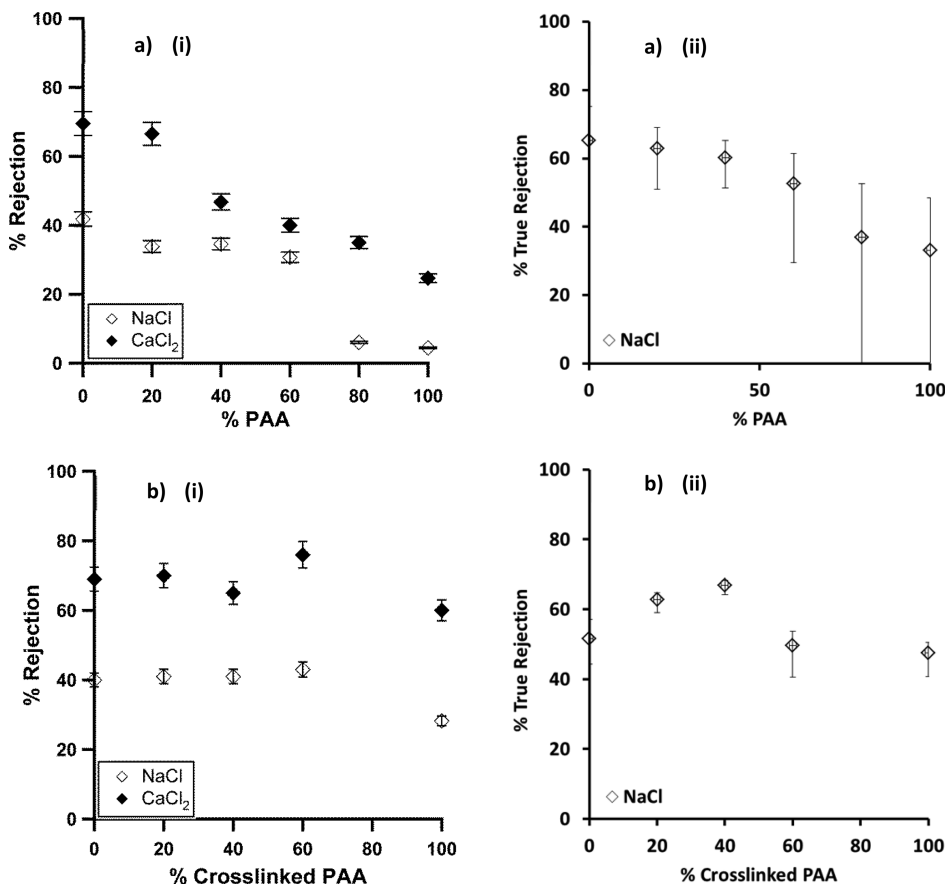


**Figure 8.** Apparent (i) and true (ii) rejection of monovalent NaCl ( $\diamond$ ) and divalent  $\text{CaCl}_2$  ( $\blacklozenge$ ) of (a) non-cross-linked and (b) cross-linked membranes with increasing PAA content in the blend solution.

unmodified PAA. As expected, membranes fabricated using the click modified polyelectrolyte displayed a more neutral membrane charge because some of the charged groups in the polyelectrolyte were replaced with cross-linking groups (Figure 5). However, in direct contrast to the unmodified PAA, the cross-linked membrane showed a significant increase in the rejection of the neutral PEG molecules with increasing PAA content. These data indicate that the use of cross-linked PAA facilitates the formation of denser polymer structures with a minimal reduction in membrane charge.

The flux measurements presented in Figure 7 show that increasing the non-cross-linking PAA content results in an overall increase in fresh water, seawater, and normalized flux, in agreement with the PEG rejection results. The salt rejection data (Figure 8a) provides further confirmation, showing that both the apparent and true rejection falls as the PAA fraction increases, reflecting a more open polymer structure.

The initial addition of 20% cross-linkable PAA to the polyanion blend causes an increase in flux that is consistent with the data for the non-cross-linkable membranes. An overall reduction in both the seawater and the fresh water flux is observed with increasing cross-linkable-PAA content, indicating a further tightening of the membrane structure. Normalized flux, indicative of salt rejection, remains constant throughout, which is further reflected in the mono and divalent salt rejection data (Figure 8b), confirming that the rejection did not improve with increasing polyelectrolyte cross-linking.

The use of PAA in the polyanion blend appears to give rise to increased membrane free volume despite an increase in

membrane negative charge, resulting in a reduction in salt rejection. With membrane cross-linking, the free volume is reduced and an increase in membrane charge is observed. However, the overall salt rejection remains steady, suggesting that cross-linking reduces the overall free volume but a reduction in the minimum pore size relevant for significant salt rejection is not observed. The blending of strongly charged PSS with a small amount of cross-linkable PAA in the polyanion blend facilitates an increase in flux with no reduction in salt rejection. These data highlight the significance of membrane-free volume over membrane charge in low to medium ion rejection cases.

## CONCLUSION

In this study, polyelectrolyte multilayer membranes were fabricated via spray-coating. Interlayer cross-linking was facilitated during deposition as opposed to post-deposition treatment via the deposition of "clickable" polyelectrolytes. Deposition of polyelectrolytes in zero salt condition appears to result in reduced coiling of the polyelectrolytes and hence a tighter pore structure and increased rejection. Addition of PAA in the polyanion blend results in increased water flux with a decrease in salt rejection, indicative of increased free volume. A change in membrane porosity under transmembrane flow of salty water is expected, as the presence of ions screens electrostatic interactions between polyelectrolyte layers, resulting in swelling. The use of cross-linkable PAA binds the polyelectrolyte structure and inhibits swelling during transmembrane flow, resulting in a reduction in the molecular weight cutoff of each membrane. By combining PSS, which gives a higher salt

rejection, with small amounts of cross-linkable PAA, which gives rise to increased flux, a significant increase in water flux with no reduction in salt rejection was observed. Ultimately, the structure of the polyelectrolyte membranes is more heavily influenced by deposition conditions and the charge density of the polyelectrolytes. The experiments reveal that polymer density is more critical than membrane charge in low to intermediate salt rejection conditions. The density and charge properties of the “click” cross-linked polyelectrolyte membranes suggests this is a suitable approach for nanofiltration, but further development is required to reach the rejection levels relevant for RO applications, especially for monovalent salts.

## AUTHOR INFORMATION

### Corresponding Authors

\*E-mail: sandraek@unimelb.edu.au.  
\*E-mail: fcaruso@unimelb.edu.au.

### Notes

The authors declare no competing financial interest.

## ACKNOWLEDGMENTS

Dr. George Q. Chen is thanked for his assistance in the determination of the concentration polarization mass transfer coefficient. The authors acknowledge support from CSIRO under the Science and Industry Endowment Fund. K.L.C. and H.L. are recipients of a John Stocker Postdoctoral Fellowship from the Science and Industry Endowment Fund. The authors also thank G.E. Water for providing the polysulfone membrane substrates used in this work.

## REFERENCES

- (1) Nicolaisen, B. Developments in membrane technology for water treatment. *Desalination* **2003**, *153*, 355–360.
- (2) Malaeb, L.; Ayoub, G. M. Reverse osmosis technology for water treatment: State of the art review. *Desalination* **2011**, *267*, 1–8.
- (3) Buonomenna, M. Nano-enhanced reverse osmosis membrane. *Desalination* **2013**, *314*, 73–88.
- (4) Lonsdale, H.; Merten, U.; Riley, R. Transport properties of cellulose acetate osmotic membranes. *J. Appl. Polym. Sci.* **1965**, *9*, 1341–1362.
- (5) Kimura, S.; Sourirajan, S. Analysis of data in reverse osmosis with porous cellulose acetate membranes used. *AIChE J.* **1967**, *13*, 497–503.
- (6) Freger, V. Nanoscale heterogeneity of polyamide membranes formed by interfacial polymerization. *Langmuir* **2003**, *19*, 4791–4797.
- (7) Roh, I. J.; Park, S. Y.; Kim, J.; Kim, C. Effects of the polyamide molecular structure on the performance of reverse osmosis membranes. *J. Polym. Sci., Part B: Polym. Phys.* **1998**, *36*, 1821–1830.
- (8) Kang, G. D.; Gao, C. J.; Chen, W. D.; Jie, X. M.; Cao, Y. M.; Yuan, Q. Study on hypochlorite degradation of aromatic polyamide reverse osmosis membrane. *J. Membr. Sci.* **2007**, *300*, 165–171.
- (9) Avlonitis, S.; Hanbury, W.; Hodgkiss, T. Chlorine degradation of aromatic polyamides. *Desalination* **1992**, *85*, 321–334.
- (10) Decher, G. Fuzzy nanoassemblies: toward layered polymeric multicomposites. *Science* **1997**, *277*, 1232–1237.
- (11) Chen, W.; McCarthy, T. J. Layer-by-layer deposition: A tool for polymer surface modification. *Macromolecules* **1997**, *30*, 78–86.
- (12) Guo, Y.; Geng, W.; Sun, J. Layer-by-layer deposition of polyelectrolyte–polyelectrolyte complexes for multilayer film fabrication. *Langmuir* **2009**, *25*, 1004–1010.
- (13) Bruening, M. L.; Sullivan, D. M. Enhancing the ion-transport selectivity of multilayer polyelectrolyte membranes. *Chem.—Eur. J.* **2002**, *8*, 3832–3837.
- (14) Bruening, M. L. Creating Functional Membranes through Polyelectrolyte Adsorption. In *Multilayer Thin Films: Sequential Assembly of Nanocomposite Materials*, second ed.; Decher, G., Schlenoff, J. B., Eds.; Wiley-VCH: Weinheim, 2012; pp 907–924.
- (15) Cheng, C.; Bruening, M. L.; Yaroshchuk, A. E. Fundamentals of selective ion transport through multilayer polyelectrolyte membranes. *Langmuir* **2013**, *29*, 1885–1892.
- (16) Qi, S.; Li, W.; Zhao, Y.; Ma, N.; Wei, J.; Wei Chin, T.; Tang, C. Y. Influence of the properties of layer-by-layer active layers on forward osmosis performance. *J. Membr. Sci.* **2012**, *423*, 536–542.
- (17) Jin, W.; Toutianoush, A.; Tieke, B. Use of polyelectrolyte layer-by-layer assemblies as nanofiltration and reverse osmosis membranes. *Langmuir* **2003**, *19*, 2550–2553.
- (18) Ariga, K.; Yamauchi, Y.; Rydzek, G.; Ji, Q.; Yonamine, Y.; Wu, K. C. W.; Hill, J. P. Layer-by-layer nanoarchitectonics: Invention, innovation, and evolution. *Chem. Lett.* **2014**, *43*, 36–68.
- (19) Sanyal, O.; Lee, I. Recent progress in the applications of layer-by-layer assembly to the preparation of nanostructured ion-rejecting water purification membranes. *J. Nanosci. Nanotechnol.* **2014**, *14*, 2178–2189.
- (20) Li, X.; De Feyter, S.; Chen, D.; Aldea, S.; Vandezande, P.; Du Prez, F.; Vankelecom, I. F. J. Solvent-resistant nanofiltration membranes based on multilayered polyelectrolyte complexes. *Chem. Mater.* **2008**, *20*, 3876–3883.
- (21) Sullivan, D. M.; Bruening, M. L. Ultrathin, gas-selective polyimide membranes prepared from multilayer polyelectrolyte films. *Chem. Mater.* **2002**, *15*, 281–287.
- (22) Qiu, C.; Qi, S.; Tang, C. Y. Synthesis of high flux forward osmosis membranes by chemically crosslinked layer-by-layer polyelectrolytes. *J. Membr. Sci.* **2011**, *381*, 74–80.
- (23) Park, J.; Kim, S. H.; Cho, J.; Bang, J. Desalination membranes from pH-controlled and thermally-crosslinked layer-by-layer assembled multilayers. *J. Mater. Chem.* **2010**, *20*, 2085–2091.
- (24) Miller, M. D.; Bruening, M. L. Correlation of the swelling and permeability of polyelectrolyte multilayer films. *Chem. Mater.* **2005**, *17*, 5375–5381.
- (25) Such, G. K.; Quinn, J. F.; Quinn, A.; Tjipto, E.; Caruso, F. Assembly of ultrathin polymer multilayer films by click chemistry. *J. Am. Chem. Soc.* **2006**, *128*, 9318–9319.
- (26) Bock, V. D.; Hiemstra, H.; van Maarseveen, J. H. CuI-catalyzed alkyne–azide “click” cycloadditions from a mechanistic and synthetic perspective. *Eur. J. Org. Chem.* **2006**, *2006*, 51–68.
- (27) Schlenoff, J. B.; Dubas, S. T.; Farhat, T. Sprayed polyelectrolyte multilayers. *Langmuir* **2000**, *16*, 9968–9969.
- (28) Krogman, K.; Zacharia, N.; Schroeder, S.; Hammond, P. Automated process for improved uniformity and versatility of layer-by-layer deposition. *Langmuir* **2007**, *23*, 3137–3141.
- (29) Ju, H.; McCloskey, B. D.; Sagle, A. C.; Wu, Y. H.; Kusuma, V. A.; Freeman, B. D. Crosslinked poly(ethylene oxide) fouling resistant coating materials for oil/water separation. *J. Membr. Sci.* **2008**, *307*, 260–267.
- (30) Sutzkover, I.; Hasson, D.; Semiat, R. Simple technique for measuring the concentration polarization level in a reverse osmosis system. *Desalination* **2000**, *131*, 117–127.
- (31) Singh, S.; Khulbe, K.; Matsuura, T.; Ramamurthy, P. Membrane characterization by solute transport and atomic force microscopy. *J. Membr. Sci.* **1998**, *142*, 111–127.
- (32) Fery, A.; Schöler, B.; Cassagneau, T.; Caruso, F. Nanoporous thin films formed by salt-induced structural changes in multilayers of poly(acrylic acid) and poly(allylamine). *Langmuir* **2001**, *17*, 3779–3783.
- (33) Stanton, B. W.; Harris, J. J.; Miller, M. D.; Bruening, M. L. Ultrathin, multilayered polyelectrolyte films as nanofiltration membranes. *Langmuir* **2003**, *19*, 7038–7042.
- (34) Miller, M. D.; Bruening, M. L. Controlling the nanofiltration properties of multilayer polyelectrolyte membranes through variation of film composition. *Langmuir* **2004**, *20*, 11545–11551.
- (35) Quinn, A.; Tjipto, E.; Yu, A.; Gengenbach, T. R.; Caruso, F. Polyelectrolyte blend multilayer films: Surface morphology, wettability, and protein adsorption characteristics. *Langmuir* **2007**, *23*, 4944–4949.